

Interaction of silane with Cu(111): Surface alloy and molecular chemisorbed phases

N. J. Curson,* H. G. Bullman, J. R. Buckland, and W. Allison

Cavendish Laboratory, Cambridge CB3 0HE, United Kingdom

(Received 7 August 1996)

Helium-atom scattering (HAS) has been used to probe the various temperature regimes of the silane/Cu(111) adsorption system. Adsorption at a surface temperature below 230 K results in the formation of chemisorbed molecular fragments with different structural regimes in the temperature ranges <165 K, 165 – 207 K, and 207 – 230 K. Growth below 165 K results in a 3×3 overlayer containing SiH_3 moieties together with SiH or Si atoms in a $P3m1$ structure. All Si atoms are bonded in threefold sites. Ordering into the final 3×3 structure occurs suddenly, near saturation coverage. Further molecular phases are observed at higher temperatures. A 4×4 phase exists between 165 and 207 K, and a second 3×3 structure occurs between 207 and 230 K. Periodicities deduced from the HAS diffraction patterns differ from low-energy electron-diffraction patterns reported previously. A gradual transition from the molecular chemisorbed phase to a surface alloy phase occurs above 230 K. The alloy phase can also be populated directly by adsorption at 400 K, resulting from the complete dissociation of the silane molecule followed by hydrogen desorption and the incorporation of silicon into the surface to give a two-dimensional hexagonal surface alloy (Cu_2Si). [S0163-1829(97)09416-2]

I. INTRODUCTION

Chemical vapor deposition (CVD) is widely used in the fabrication of thin-film devices. The appeal of the method lies in its potential to produce ultrahigh-purity overlayers and/or interfaces with submonolayer controllability and tunable characteristics. Metal-silicide interfaces produced from gas-surface reactions involving either silane or disilane are of considerable interest because of their technological importance.¹ More fundamentally, the structures formed during the CVD of silane on metal surfaces are of interest because of their novel structural properties,^{2–5} and because these systems represent prototypes that enable the elementary processes of adsorption, dissociation, and incorporation to be explored. In the case of silane/Cu(111), the various growth regimes can be followed by selective tuning of the substrate temperature.^{6–9}

Most fundamental research into the Cu-Si interface has concentrated on the growth of Cu on Si surfaces; in particular, the Cu/Si(111) system has been the subject of several studies.^{10–13} A complicated structure forms consisting of domains of different types which are quasiperiodically ordered, with the mismatched overlayer consisting of an almost planar, close-packed-hexagonal alloy of Cu_2Si . However, more recent studies of the Cu-Si interface have involved the growth of elemental silicon on Cu substrates using CVD of silane at elevated temperatures.^{2,3,6–9,14} For silane adsorption on Cu(111) above room temperature, a $(\sqrt{3}\times\sqrt{3})R30^\circ$ low-energy electron-diffraction (LEED) pattern has been observed, at saturation coverage.^{6–8} In addition, McCash *et al.*⁶ found the coverage of Si to be one-third of a monolayer. They concluded that the Si atoms occupy sites on top of the Cu surface such that they form a hexagonal overlayer. However, the observation of Si Auger peaks appearing as doublets rather than single peaks⁸ indicates that the Si atoms exist in a metal-rich environment, thus providing evidence of copper silicide formation on the surface. Recent extended x-ray-absorption fine-structure (EXAFS) studies also point to

a silicide at higher adsorption temperatures.⁹ In the related silane/Cu(001) system an incommensurate hexagonal two-dimensional Cu-Si substitutional alloy is observed.^{2,3} The Cu(111) substrate is itself hexagonal, and therefore offers a more conducive template for commensurate overlayer formation than the square mesh of the Cu(001) surface. It provides an opportunity to study the processes, such as lattice strain, that influence commensuration. Helium-atom scattering (HAS) is an ideal technique for investigating the nature of such a surface because it provides details about the surface corrugation (as well as surface symmetry), which is expected to differ significantly for surfaces comprising of two-dimensional alloys and of ordered adsorbates. In particular, the HAS technique is uniquely sensitive to the presence of hydrogen within the region of the surface.

Few studies of silane on Cu(111) at low temperatures have been reported^{6–9} and these have yet to yield a coherent picture of the adsorption process. At ~ 100 K, the silane molecule undergoes partial molecular dissociation, and at saturation coverage the surface exhibits a $(\sqrt{3}\times\sqrt{3})R30^\circ$ LEED pattern.^{6,7,9} However, the extent to which the dissociation occurs and which of the silyl species (SiH_n , $n=1-3$) are subsequently resident on the surface, is disputed. Other experiments,⁸ using Fourier transform infrared spectroscopy and thermal-desorption spectroscopy (TDS), suggest that the overlayer is comprised of SiH_2 and SiH moieties, whereas studies using electron-energy-loss spectroscopy (EELS) and reflection-adsorption infrared spectroscopy (RAIRS),⁶ and EXAFS and x-ray-absorption near-edge spectroscopy,⁷ have concluded that a single species exists on the surface, with SiH_3 the most likely candidate.

The results presented below reveal that either a surface alloy phase or a molecular chemisorbed phase can be formed on the surface, by appropriate tuning of the substrate temperature. The molecular chemisorbed phase is shown to have three structural regimes, each associated with a different substrate temperature range. For substrate temperatures below 165 K, the presence of SiH_3 moieties on the surface is con-

firmed (and a structure proposed), thus resolving an issue of contention within the literature.⁶⁻⁸ The surface alloy phase is shown to have a hexagonal Cu_2Si structure, and the results provide a valuable insight into the energetics of surface alloy formation. The main emphasis of the paper is to present a structural study of the silane/ $\text{Cu}(111)$ interface for the molecular chemisorbed phase below 165 K, and the surface alloy phase.

II. EXPERIMENT

The experiments were performed in a purpose-built ultrahigh-vacuum chamber with a base pressure of below 1×10^{-10} mbar. The helium beam had an energy of 71 meV, and was produced by supersonic expansion.¹⁵ Scattered atoms were detected using a quadrupole mass spectrometer (overall angular resolution $\sim 0.4^\circ$) located in a movable, differentially pumped chamber. A six-axis sample manipulator was used to position the sample accurately with respect to the incident helium beam and the detector. The $\text{Cu}(111)$ single crystal was prepared by mechanical polishing and chemical etching before use. In vacuum, the sample was cleaned by repeated cycles of argon-ion bombardment ($\sim 2.5 \mu\text{A cm}^{-2} \text{Ar}^+$ at 500 V), and annealing to 700–750 K until only a narrow intense specular helium scattering peak was observed. The ion-bombardment and annealing of the sample was performed before each exposure of the $\text{Cu}(111)$ surface to silane. The sample temperature was varied by liquid-nitrogen cooling together with electron bombardment, and monitored with a Cr-Al (*K* type) thermocouple spot-welded next to the crystal, giving an accuracy estimated to be better than ± 5 K. Silane exposure was carried out at 2×10^{-6} mbar (total measured pressure) using a 0.5% silane in argon mixture. The silane gas dilution was taken into account when calculating the silane exposure.

III. TEMPERATURE DEPENDENCE OF SILANE/ $\text{Cu}(111)$ INTERACTION

The rearrangements occurring on a surface can be conveniently studied as a function of surface temperature, using helium-atom scattering. This is done by simply monitoring the specular intensity of the helium beam (scattered off the surface) as a function of linearly increasing surface temperature (temperature programmed scan). Debye-Waller effects cause a gradual and predictable change in the specular intensity as the temperature changes in a temperature programmed scan. However, more sudden changes in the specular intensity can be caused by a structural rearrangement of the surface. This is because the helium intensity scattered from a surface, into the specular beam, increases as a function of increasing surface order and as a function of decreasing surface corrugation.¹⁶ Since any structural rearrangement of a surface is likely to affect both the corrugation and the degree of surface order, sharp changes in the gradient of the specular intensity during linear heating of the surface indicate that the surface has undergone a structural change.

The various regimes of structural change have been identified by monitoring the specularly scattered helium atoms during a temperature-programmed experiment. Figure 1 shows the results from a sample dosed with SiH_4 to satura-

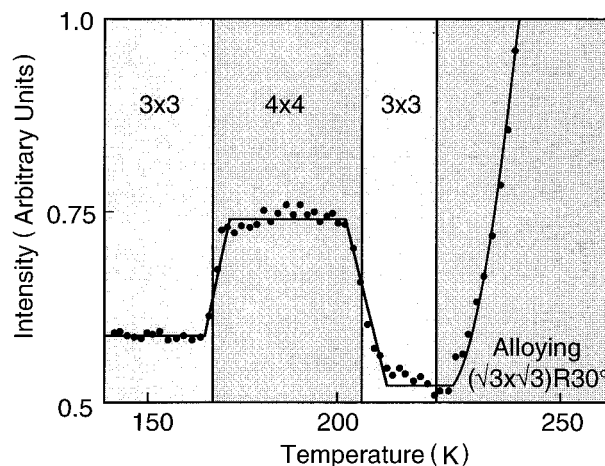


FIG. 1. Temperature programmed scan in which the specular intensity of the helium beam is monitored as the surface temperature is increased linearly with time. The initial surface was obtained by adsorbing silane on $\text{Cu}(111)$ below 150 K, to saturation. Changes in structure, indicated by a variation in the intensity, are shown. The solid curve is a guide to the eye.

tion at an adsorption temperature of 150 K. The sample was then heated at a rate of 0.25 K/s while the intensity of the specular helium beam was monitored. The change in intensity due to the Debye-Waller effect has been subtracted from the data. A number of distinct changes are apparent in Fig. 1. At 165 K there is an increase in the specular intensity, and, at 207 K, the specular intensity undergoes a distinct decrease. Structural rearrangements of the surface occur at both of these temperatures. The surface undergoes a third structural change at 230 K, where a minimum in the specular intensity is seen. There follows a gradual but large intensity rise, with the intensity reaching a maximum (not shown) without any further sudden changes. The intensity at the maximum is 25 times greater than the initial intensity at 150 K, implying that above 230 K the surface undergoes a considerable decrease in corrugation and/or increase in order. All of the structural changes observed in Fig. 1 are irreversible.

It was found from HAS diffraction patterns (described below) that ordered structural phases did indeed exist in the following regimes of substrate temperature, T_s : $T_s < 165$ K, $165 \text{ K} < T_s < 207$ K, and $207 \text{ K} < T_s < 230$ K. An ordered surface was also seen to develop gradually above 230 K. The observed unit-cell designation of the various phases are indicated in Fig. 1, and those for $T_s < 165$ K and $T_s > 300$ K are discussed later in the paper. The structural transitions were irreversible as determined by the fact that once the surface temperature had been raised to a particular regime, the structure associated with that regime remained, even when the sample temperature was lowered again.

We find that the gradual surface rearrangement above 230 K in Fig. 1 marks the transition from a molecular chemisorbed phase seen at lower temperatures, to a surface alloy phase. It is found that there are different chemical processes involved in the formation of the two phases. The surface alloy phase results from the processes of complete molecular dissociation, desorption, and incorporation growth (up to the formation of a single-monolayer film). The molecular chemisorption phase results from the processes of partial molecular

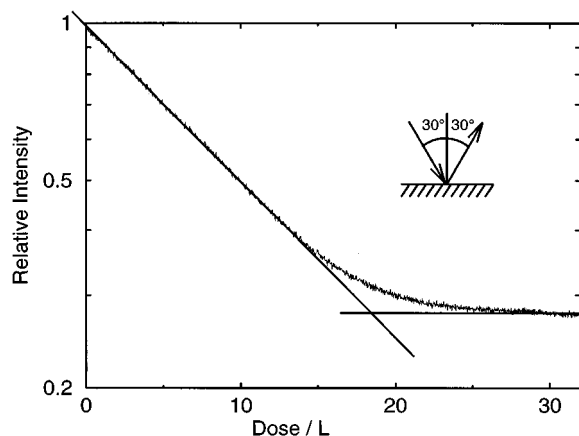


FIG. 2. Specular helium scattering during silane adsorption (on a log scale) as a function of dose, at 400 K. The lines are drawn to emphasize the deviation of the curve from straight-line behavior. The angle of incidence of the helium was 30° , and the beam energy was 71 meV.

dissociation and chemisorption (of the dissociation products). The latter phase consists of three separate structural regimes (within the temperature range investigated), with the energetically preferred regime depending critically on sample temperature. The different phases are now discussed in turn, starting with the alloy phase.

IV. SURFACE ALLOY PHASE

The surface alloy phase is formed either by silane adsorption at 400 K or by silane adsorption at lower temperatures followed by annealing of the surface to 400 K. It is known from previous studies that silane undergoes complete molecular dissociation on Cu(111) at elevated temperatures.^{6,8} TDS studies¹⁷ have shown that the desorption temperature of hydrogen on Cu(111) is ~ 290 K. Consequently, adsorption of silane on Cu(111) at 400 K results in a surface consisting of Si and Cu atoms. However, the nature of the adsorption process has been disputed. McCash *et al.*⁶ suggested that chemisorption occurred with Si atoms residing atop the Cu surface. In contrast, Wiegand, Lohokare, and Nuzzo⁸ predicted the formation of a copper silicide surface alloy. To resolve this issue we performed HAS experiments during and after the growth at 400 K.

Figure 2 shows the development of the specularly scattered helium intensity during the adsorption of silane on Cu(111) at 400 K. The specular intensity decreases continuously from the initial value corresponding to the mirrorlike Cu(111) surface, and saturates at approximately 0.26 of the initial intensity. The absence of oscillations and the significant intensity at saturation enable us to rule out the possibility of layer-by-layer growth¹⁸ and the growth of three-dimensional islands,¹⁹ respectively. The most likely growth mode is the formation of a single monolayer, after which the sticking probability for further silane molecules becomes vanishingly small. This conclusion is supported by Auger-electron spectroscopy data,⁶ which indicate that the saturation coverage was less than one monolayer.

The initial gradient in Fig. 2 gives a cross section, for each Si atom, of approximately $\sim 10 \text{ \AA}^2$, much smaller than

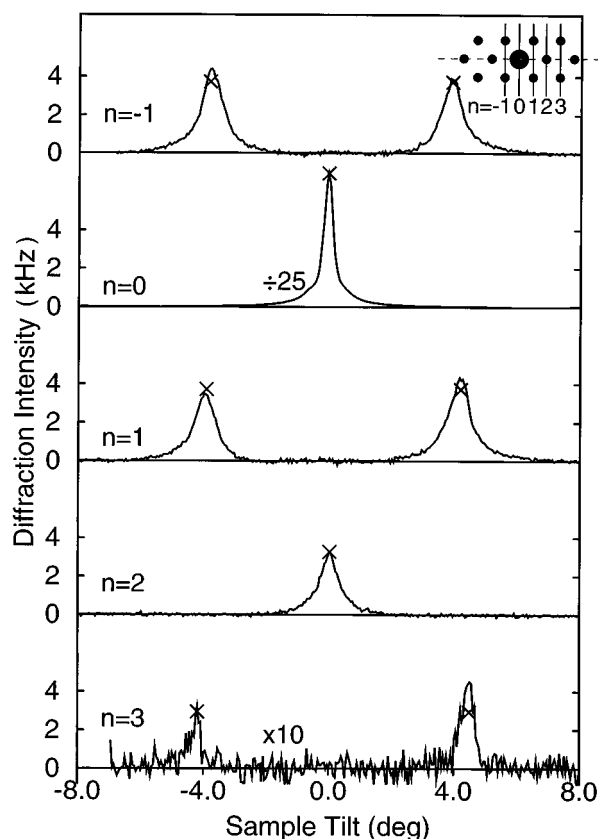


FIG. 3. Measured and calculated helium-diffraction intensities obtained from the silane/Cu(111) saturated surface, formed at 400 K. The saturated surface was cooled to 150 K before the diffraction scans were performed. The full curves are experimental measurements, and the crosses (x) are calculated values after fitting to the integrated intensities under the experimental peaks and accounting for the incoherently scattered background. The inset shows a schematic of the $(\sqrt{3} \times \sqrt{3})R30^\circ$ diffraction pattern with the (00) peak indicated by a large circle. The direction, in reciprocal space, of each scan is indicated by vertical solid lines. The dotted horizontal line shows the peaks corresponding to diffraction in the plane defined by the incident beam and detector. For all the latter peaks, $\theta_i = 30^\circ$. The energy of the incident beam was 71 meV.

is typical for isolated atomic or molecular adsorbates. Also, the relatively high specular intensity of the saturated structure indicates that the corrugation induced by Si is weak. These qualitative observations are the first indication that silicon atoms are incorporated in the overlayer rather than adsorbed on the substrate. We now describe a quantitative structural study, which confirms that a two-dimensional (2D) alloy phase is formed.

Helium diffraction spectra, following a saturation silane exposure at 400 K, are shown in Fig. 3. The scans were recorded after cooling to a surface temperature of 150 K. In each scan the detector position is fixed and the surface normal is tilted out of the scattering plane. ΔK_y is varied at a fixed ΔK_x , as indicated by the vertical lines in the inset to the figure. The strongest peak in the diffraction pattern corresponds to specular scattering at a total scattering angle of 60° ($\theta_i = \theta_f = 30^\circ$). The sharpness of the peaks in Fig. 3 (the full width at half maximum of the specular peak is similar to that of the clean surface) and low diffuse background sug-

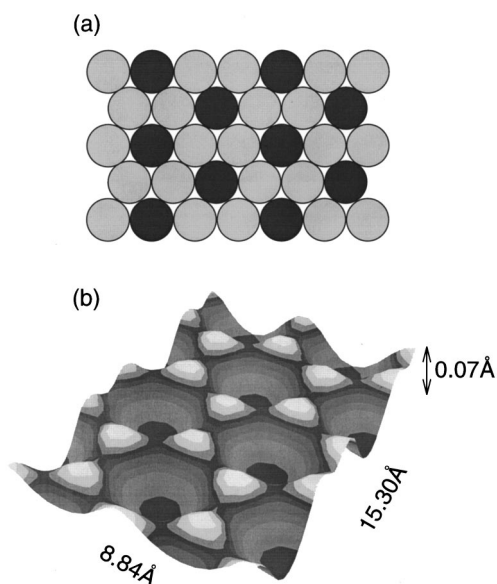


FIG. 4. (a) Schematic view of the Cu_2Si structure where $\frac{1}{3}$ ML of substrate atoms are replaced by Si atoms (darker shading) to form a two-dimensional hexagonal surface alloy. (b) The best-fit corrugation for the surface produced by silane adsorption on Cu(111) at 400 K, to saturation. The height scale has been exaggerated for clarity. The corrugation was obtained by representing $\frac{2}{3}$ ML of surface atoms by Gaussian functions whose height and width were optimized to give the best fit between experimentally measured and theoretically calculated diffraction intensities. The optimized parameters of the fit were Gaussian heights of 0.07 \AA and widths of 2.11 \AA .

gests that the saturated surface is well ordered. This, in turn, indicates that the reduction in specular scattering from the saturated surface in comparison to the clean Cu(111) surface is related to an increase in surface corrugation. The diffraction pattern reveals the unit cell of the saturated surface to have a $(\sqrt{3} \times \sqrt{3})R30^\circ$ symmetry, in agreement with previous LEED observations.^{6,7}

The analysis of the diffraction data to yield a surface corrugation was aided by the independent assignment of the saturation coverage of Si to be one-third of a Cu(111) monolayer, determined by Auger-electron spectroscopy.⁶ Determination of the surface corrugation involves the calculation of the intensity of diffraction peaks obtained from suitably chosen model surfaces, and then comparison of these intensities with the experimentally measured diffraction intensities. The calculations utilized the eikonal approximation for hard-wall scattering which is valid given the high beam energy and low angle of incidence used (71 meV , 30°).²⁰

The hard-wall corrugation function was constructed from radially symmetric Gaussian functions centered on Cu sites (i.e., $\frac{2}{3}$ ML of atoms) in a $(\sqrt{3} \times \sqrt{3})R30^\circ$ arrangement. Identical Gaussians were used, and this gives two adjustable parameters (height and radius) to fit the diffraction intensities.^{20,21} A simple nonlinear χ^2 minimization was used. The resulting corrugation function is shown in Fig. 4(b), and the corresponding surface structure in Fig. 4(a). The most prominent feature in the corrugation function is a small hollow of $\sim 0.07 \text{ \AA}$ depth.^{22,23} We attribute the hollow to Si atoms, in a 2D alloy, surrounded by a hexagon of Cu atoms, which have a slightly larger covalent radius.

The low surface corrugation is not consistent with an on-top adsorption system, whose corrugation would be significantly greater. For example, adsorption of O_2 on Ni(111) (Ref. 24) and Pb on Cu(001) (Ref. 25) results in corrugations of 0.5 and 4 \AA , respectively. The surface corrugation of 0.07 \AA deduced from the present diffraction patterns is only consistent with a 2D surface alloy. Thus we conclude that the adsorption of silane on Cu(111) at 400 K produces a substitutional surface alloy with silicon atoms becoming incorporated into the top layer of the copper substrate. This determination of a 2D Cu_2Si structure shown in Fig. 4(a) is supported by the fact that the two-dimensional alloys formed by the Si/Cu(001) and Cu/Si(111) systems are also Cu_2Si .

A similar corrugation function is obtained if the radial Gaussian functions are centered on Si sites (i.e., $\frac{1}{3}$ ML of atoms) in the same $(\sqrt{3} \times \sqrt{3})R30^\circ$ arrangement. Again there are two adjustable parameters, and the fit gives a corrugation dominated by a hollow of depth $\sim 0.07 \text{ \AA}$. Although the corrugation functions are very similar, the fits differ at the 99% confidence level, with the model using Cu atoms being the better of the two. The difference between the two corrugation functions lies in a small, but evidently significant, corrugation around the rim of the Si hollow. The corrugated hexagonal rim of Cu atoms is clearly visible in Fig. 4(b). The observation of some corrugation in the metal atoms contrasts with the original Cu(111) surface, which shows no corrugation. Significant changes in the nature of the metallic bonding must have taken place with the incorporation of Si atoms into the surface layer.

A comparison between the results described above and those of an earlier study of silane adsorption on Cu(001) (Refs. 2 and 3) provides an insight into the competing processes that determine how a two-dimensional alloy overlayer is accommodated on a surface. The 2D surface alloys formed by silane CVD on both Cu(111) and Cu(001) have similar hexagonal Cu_2Si structures. However, the response of the two overlayer systems to stress within the alloy surface is quite different. Two factors determine the total energy of the system. (1) *Commensuration*: The driving force for commensuration is the positioning of overlayer atoms with respect to substrate atoms in a way that favors optimum overlayer-substrate bond formation. This bond formation lowers the total surface energy. (2) *Bond length/angle deformation*: A hexagonal Cu_2Si overlayer will ideally have in-plane bond angles of 120° , and bond lengths determined by the covalent radii of the Cu and Si atoms. For these ideal values of bond length and angle, the strain energy of the overlayer will be at a minimum. Any deformation of these lengths or angles upon interaction with the substrate will result in an increase in strain energy, and thus an increase in total surface energy. Alternatively the strain energy can be considered as arising from a deviation from ideal overlayer density. As the density is increased (decreased) by the compression (stretching) of in-plane bonds, then the strain energy is increased.

The Cu(111) and Cu(001) surfaces provide hexagonal and square meshes, respectively, for silane adsorption. In the case of Cu(111) the outermost layer of Cu atoms has the same basic structure (hexagonal) as the Cu_2Si overlayer. Although the density of the ideal 2D Cu_2Si layer is greater than that of the substrate (the Si covalent radii is $\sim 10\%$ smaller than that of Cu), the mismatch is insufficient to generate a

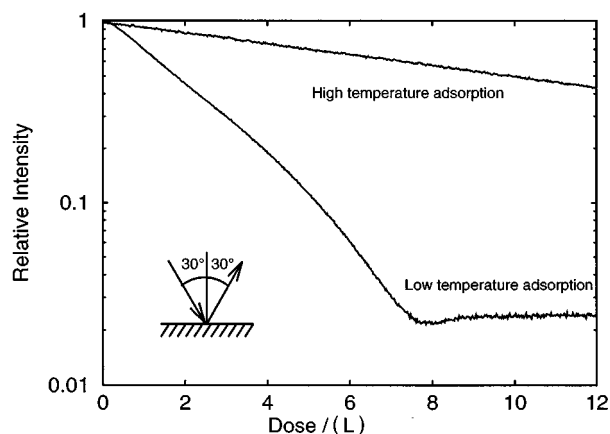


FIG. 5. Specular helium scattering during silane adsorption on Cu(111) at 150 K (lower curve). The partial pressure of silane gas was 1×10^{-8} mb. The corresponding uptake curve for adsorption at 400 K is also shown, although in this case the surface does not saturate until approximately 30 L. The angle of incidence of the helium was 30° , and the beam energy was 71 meV.

reconstruction, and a commensurate structure is observed. The energy gain from commensuration outweighs the increase in strain energy caused by stretching of the in-plane bonds and by the decrease in overlayer density.

Graham and co-workers^{2,3} found that silane adsorption on the square mesh of the Cu(001) surface produced an incommensurate Cu_2Si overlayer whose registry with the substrate was complicated. For the $\text{Cu}_2\text{Si}/\text{Cu}(001)$ adsorption system, the minimum surface energy is obtained by the retention of near-ideal in-plane bond angles within the Cu_2Si overlayer, and by the increase of the Cu_2Si overlayer density, at the expense of the loss of overlayer registry with the substrate. The structure of the incommensurate system has some similarities with the surfaces of Pt(001) and Au(001), which also reconstruct to give quasihexagonal overlayers. The corresponding hexagonal surfaces of Pt(111) and Au(111) are known to reconstruct;²⁶ however, there is no corresponding analogy with the case of the $\text{Cu}_2\text{Si}/\text{Cu}(111)$ system, since the surface stress in the latter system is not enough to generate a reconstruction.

V. MOLECULAR CHEMISORBED PHASES

This section describes our investigation into silane adsorption on the Cu(111) surface in the three temperature regimes below 230 K, identified in Sec. III, i.e., <165 K, 165–207 K, and 207–230 K. The possible adsorbates include silyl fragments and atomic hydrogen. Our investigation of the molecular chemisorbed phase places most emphasis on the structures occurring at 150 K, where partial molecular dissociation of the silane molecules has been predicted, but where the degree of dissociation has been the cause of some dispute.^{6–9}

Figure 5 shows the specular helium intensity during the adsorption of silane on Cu(111) at 150 K. The equivalent curve for the surface alloy phase is shown for comparison, although it should be noted that for adsorption at 400 K the surface is not saturated after a dose of 12 L (Fig. 2 shows the complete 400-K uptake curve). The intensity decrease upon

adsorption and the subsequent saturation of the surface, for adsorption at 150 K, occur over a much shorter time scale compared with adsorption at 400 K. The rapid initial decrease in specular intensity shows that the scattering cross section of the adsorbed species is larger at 150 K, i.e., silyl moieties are adsorbed as opposed to Si atoms. The shorter time to saturation shows that the sticking coefficient is greater at 150 K, and/or the saturation coverage is lower.

Another interesting difference between the two growth curves in Fig. 5 is the form of the curves at low coverages. The 400-K uptake curve closely conforms to the exponentially decreasing behavior expected for the adsorption of noninteracting adsorbates²⁷ (up to an exposure of 20 L), whereas for adsorption at 150 K the decrease in specular intensity soon becomes more rapid than that of an exponential decay. The most likely explanation for this change in slope is the existence of a repulsive interaction between adsorbates,²⁷ causing the adsorbates to occupy a maximum surface area and consequently minimizing their scattering cross-section overlap. This explanation, which is evidence of adsorption on top of the surface, is strongly supported by the coverage-dependent diffraction scans presented later in the paper.

Further evidence of a fundamental difference in the adsorption processes of the molecular chemisorbed and surface alloy phases is highlighted by the fact that the 150-K uptake curve goes through a minimum before saturation coverage is reached. This minimum indicates that during growth the surface reaches a maximum state of disorder (at the minimum), and then abruptly reorders to form the saturated surface. The origin of the reordering process is discussed in more detail later.

As with the surface alloy phase, the fact that the specular intensity approaches a constant final value suggests that the surface at 150 K has become saturated. Again there is no evidence of layer-by-layer or three-dimensional island growth. However, the growth curve at 150 K shows a considerably lower saturated intensity than at 400 K, with the specular intensity falling from the clean surface value by 96% compared with 73% at 400 K. Diffraction scans taken from the 150-K saturated surface and shown in Fig. 6(a) indicate that the quality of surface order (determined by comparison of peak widths and diffuse background) is similar to that of the 400-K surface. However the scans in Fig. 6(a) have significantly larger rainbow angles and greater $I_{\text{diff}}/I_{\text{spec}}$ ratios than those of Fig. 3, demonstrating that the corrugation of the surface after adsorption at 150 K is indeed significantly greater than after adsorption at 400 K, supporting our assignments of molecular chemisorbed and surface alloy phases, respectively.

Figure 6(b) shows a composite view of the intensities and positions of the diffraction peaks in Fig. 6(a). Each spot in the diagram represents a diffraction peak, and the area is proportional to the integrated intensity of the peak. Information obtained from the peak intensities is discussed below. The positions of the diffraction peaks in reciprocal space reveal a 3×3 diffraction pattern. The surface periodicity observed by helium-atom scattering is different from the $(\sqrt{3} \times \sqrt{3})R30^\circ$ diffraction pattern observed by two independent studies^{6,7} using LEED. The observation of different LEED and HAS diffraction patterns from the same surface

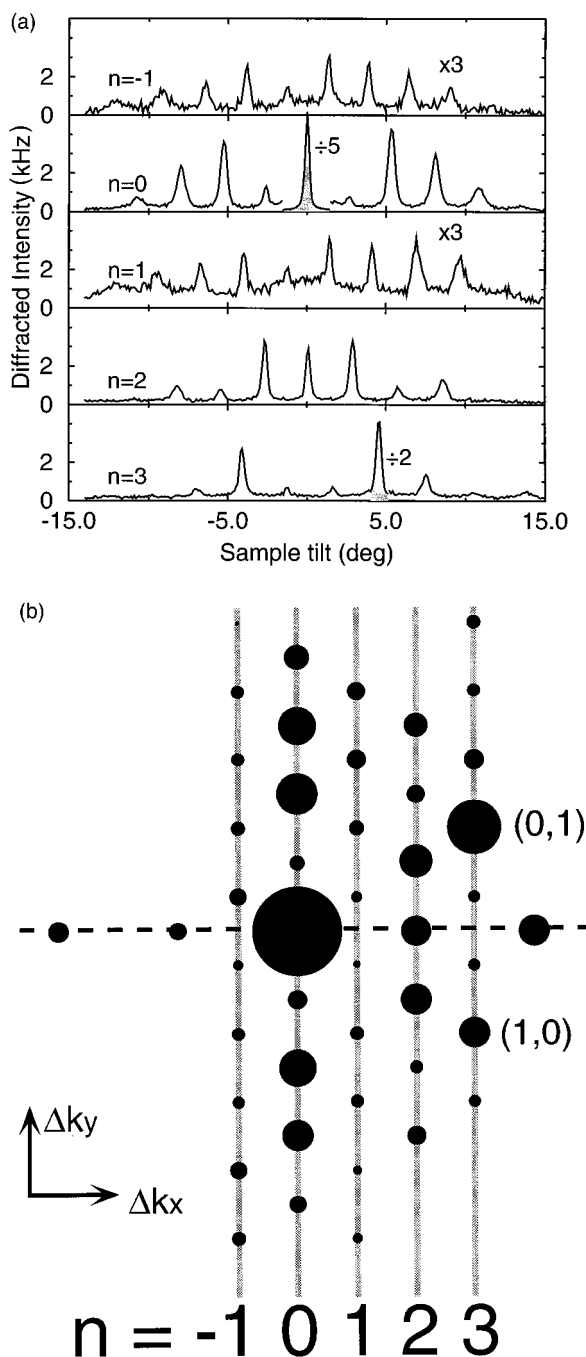


FIG. 6. (a) Measured helium-diffraction intensities obtained from the silane/Cu(111)-saturated surface, formed at 150 K. The scattering geometry is the same as in Fig. 3. Shaded peaks have been scaled down as indicated. (b) HAS diffraction pattern constructed from the scans shown in (a). Each spot represents a diffraction peak with the area of the spot proportional to the integrated intensity of the peak. The dotted line indicates scattering in the plane defined by the incident beam and the detector.

structure is not uncommon,²¹ and originates from the fact that helium atoms diffract from the outermost charge density of a surface, whereas electrons diffract from the heavy ion cores of atoms in the first few layers of a surface. One consequence of the fundamental difference in scattering processes is that LEED is only weakly sensitive to hydrogen atoms (whether directly bonded to the surface or present on

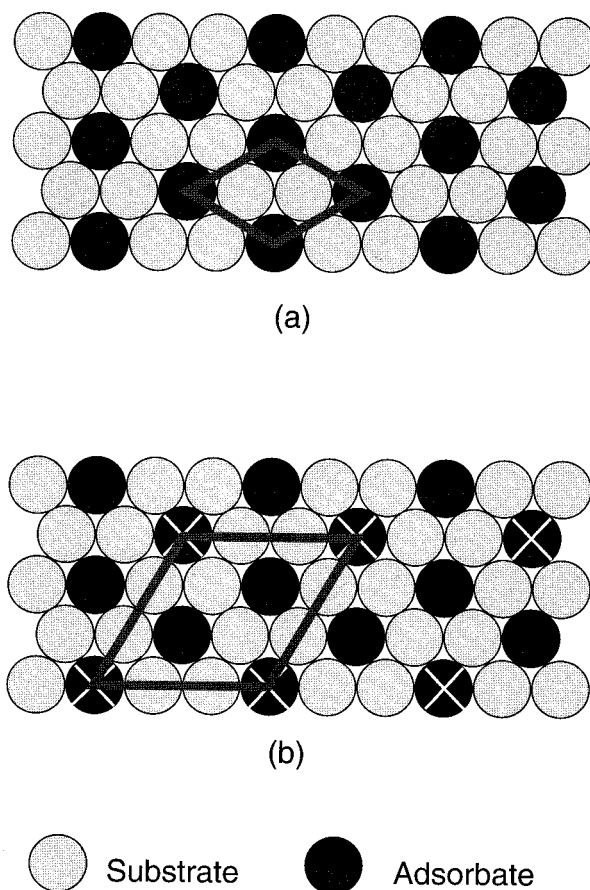


FIG. 7. Schematic diagram showing positions of adsorbates required to produce (a) a $(\sqrt{3} \times \sqrt{3})R30^\circ$ LEED diffraction pattern and (b) both a $(\sqrt{3} \times \sqrt{3})R30^\circ$ LEED diffraction pattern and a 3×3 HAS diffraction pattern. Adsorbates marked with the cross must scatter electrons in the same manner as the other adsorbates, but appear different when scattering helium atoms. A $(\sqrt{3} \times \sqrt{3})R30^\circ$ unit cell is outlined in (a), and a 3×3 unit cell is outlined in (b).

the surface as part of a molecule), whereas the sensitivity of HAS to hydrogen will depend on the extent to which the hydrogen atoms contribute to the corrugation of the surface charge density.²¹

For silane adsorption on Cu(111) at low temperature, the superlattice peaks observed by LEED will originate primarily from the scattering of electrons from an ordered arrangement of silicon atoms. Hydrogen atoms will contribute significantly less intensity. The silicon atoms could be components of silyl fragments or individual silicon atoms. If all these silicon containing species were identical, then the HAS diffraction pattern would also be $(\sqrt{3} \times \sqrt{3})R30^\circ$; however, the fact that the HAS pattern is of higher order (i.e., 3×3) than the LEED pattern shows that not all the silicon-containing species are the same. Figures 7(a) and 7(b) show the unit cells indicated by the LEED and HAS results, respectively. As Fig. 7(b) shows, the silicon-containing species at the corners of the 3×3 unit cell must be identical to satisfy both LEED and HAS results. The other two silicon-containing species within the 3×3 unit cell must be different to the first in a way that HAS can distinguish but LEED

cannot. It naturally follows that the difference between species within a unit cell is a difference in the nature of the hydrogen atoms which are part of those species, i.e., there must be different silyl moieties within a unit cell (the species differ in the numbers of hydrogen atoms they contain, $n=0-3$) or there could be the same silyl moieties but with different rotational orientations or a combination of both differences.

Previous studies of silane adsorption on Cu(111) have failed to agree on which silyl moieties reside on the surface in the low temperature regime. The RAIRS spectra obtained by McCash *et al.*⁶ contained relatively few adsorption peaks indicating that only one silyl species was present on the surface at 101 K. The results (along with EELS data) were interpreted as providing evidence for either SiH₂ or SiH₃ adsorption. It was concluded by McCash *et al.* that SiH₃ was the most likely adsorption species by comparison with methane adsorption on metal surfaces.

A significantly different conclusion about the low temperature silane/Cu(111) surface has been proposed by Wiegand, Lohokare, and Nuzzo⁸ on the basis of Fourier-transform infrared spectroscopy (FTIRS) and temperature programmed reaction spectroscopy (TPRS). The FTIRS spectra contained more peaks at saturation than were seen in the RAIRS spectra of McCash *et al.* and some of the peaks were assigned to different vibrational modes. In Ref. 8 it was concluded that the surface consisted of SiH moieties at low coverage and SiH and SiH₂ moieties at saturation coverage.

Important clues to the surface structure can be obtained from a consideration of the symmetry features in the observed diffraction pattern. In particular we note the absence of any mirror plane in Fig. 6(b). The fact that the HAS diffraction pattern was obtained using a non-normal incidence beam (30° in this case) means that the perpendicular momentum transfer will vary in the plane of the incident beam. The intensity of two symmetrically equivalent peaks will only be the same when the value of the perpendicular momentum transfer of the incident atoms is the same for both peaks. Thus the only mirror plane expected is that containing the scattering plane and the surface normal, as indicated by the dotted line in Fig. 6(b). Peaks such as (10) and (01), or ($\frac{1}{3}$ 0) and (0 $\frac{1}{3}$), demonstrate clearly the absence of this mirror plane. Note that peak intensities are proportional to area of the spots in Fig. 6(b); thus the difference between the (01) and (10) intensities corresponds to a factor of approximately 3. We conclude that the surface does not have sixfold symmetry. Either the surface consists of a single domain with threefold symmetry, or there are three unequal domains of *P1* or *P3* symmetry. We rule out the possibility of three unequal domains on the basis of the very strong asymmetry in intensities across the scattering plane. Only three of the diperic space groups remain to be considered:²⁸ DG65 (*P3*), DG69 (*P3m1*), or DG70 (*P31m*) symmetry. Of these, the *P31m* symmetry can be ruled out because of the missing mirror plane.

The fact that the symmetry of the surface structure is *P3* or *P3m1* allows us to rule out immediately one of the proposed structural models for the 150-K saturated silane/Cu(111) surface. The surface must contain elements of threefold point-group symmetry (to generate a single-domain surface of threefold symmetry). The model of Ref. 8 consists

of SiH₂ and SiH moieties. An ordered arrangement of SiH₂ and SiH moieties, with their Si atoms positioned within the requirements of Fig. 7, cannot form a threefold structure. In contrast, McCash *et al.*'s prediction of a surface consisting of SiH₃ moieties (which have threefold point-group symmetry) is not ruled out.⁶

We have analyzed the diffraction pattern starting with trial surface corrugations. Since there were several possible adsorption species (i.e., SiH_{*n*} with $n=1-3$, Si, and H) and many combinations of these species, our objective has been to gain quantitative information about the position and molecular orientation of the silyl fragments rather than obtain a complete structural model. For this purpose we have made use of Patterson synthesis, which emphasizes particular positional correlations. The generation of structural models was based on strong features in the experimental Patterson function. Trial corrugations were subsequently generated as described in Sec. IV and their HAS diffraction intensities were calculated exactly.^{29,30} For the modeling of silyl moieties, it was the hydrogen atoms of these molecules that were represented by Gaussians, since the hydrogen atoms extend outwards from the surface and away from the silicon atoms to which they are bonded. The H-H distances within the silyl moieties were estimated from typical Si-H bond lengths.³¹

A modification of the method of Patterson synthesis (normally used for x-ray diffraction) can be applied to HAS because of the close relationship between the structure factor of kinematic diffraction theory in standard three-dimensional crystallography and the eikonal approximation used in atomic beam diffraction from surfaces.³² The conventional Patterson function gives a correlation function of electron density while, in the case of helium scattering, the Patterson function we determine from the data is a correlation function of scattering phases. Within the hard-wall approximation the Patterson function is equivalent to a correlation function of surface heights in the surface electron density. The continuous distribution of the scattering centers seen by HAS is responsible for the fact that HAS yields Patterson functions with less intense peaks and higher background than in conventional x-ray diffraction.

Figure 8(a) shows the Patterson function obtained from the experimentally determined diffraction intensities [Fig. 6]. Figure 8(b) shows the Patterson function obtained from the diffraction intensities calculated from the best-fit corrugation that the trial corrugations produced. The structural model corresponding to the best-fit corrugation is shown in Fig. 9. The Patterson functions show trivial origin peaks at the corners of the primitive cell, and a number of other distinct Patterson peaks which are labeled 1-6. Each of the other peaks is symmetrically equivalent to one of the labeled peaks. Figure 8(c) demonstrates where the peaks in Figs. 8(a) and 8(b) originate by showing the interatomic vectors that exist in a primitive unit cell of the proposed structure. The numbers shown next to the vectors in Fig. 8(c) indicate the correspondence between peaks shown in Figs. 8(a) and 8(b).

A number of trial structures were modeled and tested, including all possible structures inferred from previous work.⁶⁻⁹ Figure 9 shows the only model structure whose Patterson function reproduced the Patterson function obtained from experimentally measured diffraction intensities. The structure in Fig. 9 consists of two SiH₃ moieties with

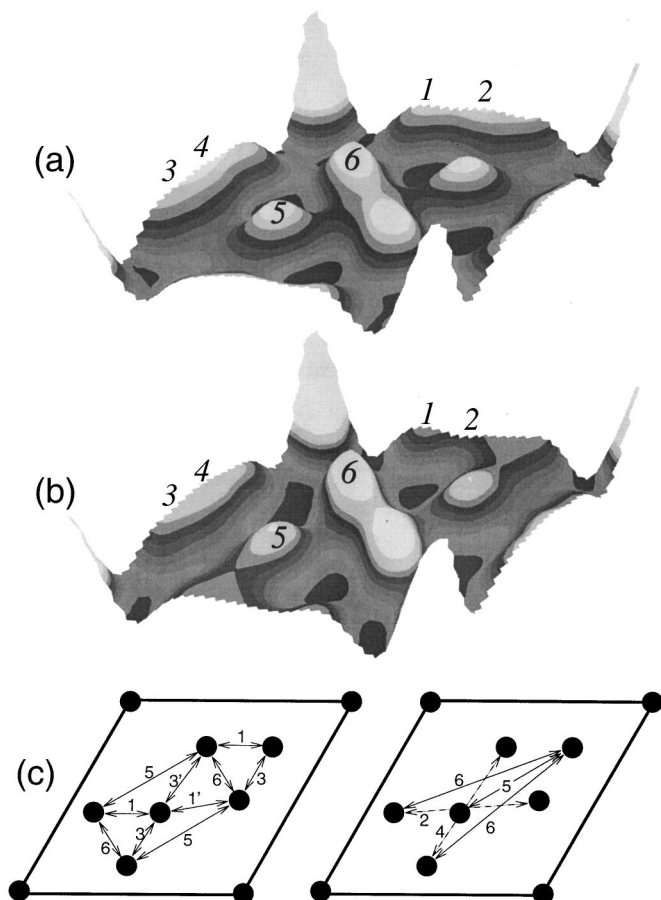


FIG. 8. (a) and (b) show the Patterson functions obtained from the experimentally determined diffraction intensities and from the diffraction intensities calculated from the model surface of Fig. 9, respectively. The areas of (a) and (b) correspond to the primitive unit cell shown in Fig. 9. The Patterson functions show trivial origin peaks at the corners of the unit cell. Other distinct Patterson peaks are labelled 1–6. Vectors corresponding to each peak are shown in (c). Unmarked peaks are symmetrically equivalent to one of the labeled peaks.

the same rotational orientation, and one other moiety which has a C_∞ point group. This second moiety could be elemental silicon or SiH, but atomic hydrogen is ruled out on the basis of LEED data, as discussed above. The structure was modeled with the SiH (or Si) atoms and the hydrogen atoms of the SiH₃ moieties represented by Gaussians of height 0.25 Å and width 1.5 Å.

The space group of the proposed structure is $P3m1$. Related models with $P3$ symmetry (i.e., with low symmetry configurations for the SiH₃ features) do not generate Patterson functions that are consistent with the experimental data. The proposed structure maximizes the distances between hydrogen atoms, suggesting a repulsive H-H interaction. It is assumed that all Si atoms in the unit cell have the same adsorption site in order that the $(\sqrt{3} \times \sqrt{3})R30^\circ$ LEED pattern is satisfied. However, that site cannot be an on-top site or a bridge site. If it were, then several domains of the structure shown in Fig. 9, with different SiH₃ orientations, would exist on the surface. A combination of these domains would yield a diffraction pattern with higher symmetry, at variance with the observed HAS diffraction intensities. An overlayers

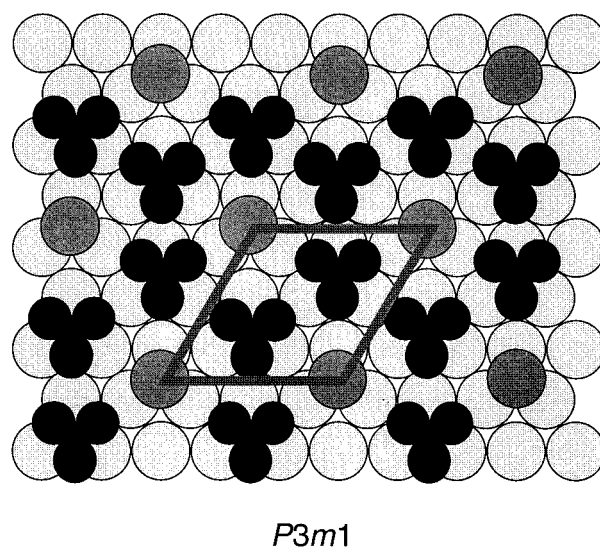


FIG. 9. The proposed structural model for the saturated silane/Cu(111) surface, formed at 150 K. The structure consists of two SiH₃ moieties per unit cell (shown black) with either SiH or elemental silicon (dark shaded circles) at the corners of the primitive unit cell. A primitive unit cell is highlighted by the full lines. The structure has $P3m1$ symmetry, and the structure maximizes the distance between hydrogen atoms.

consisting of a single domain of the proposed structure (i.e., with SiH₃ triangles only pointing in one direction) can be rationalized only if the SiH₃ moieties are adsorbed on threefold hollow sites, as shown in Fig. 9. It can be seen that if the SiH₃ moieties are rotated by 30° (so the triangles are pointing upwards) then the hydrogen atoms will be positioned above atoms from the Cu top layer instead of above threefold hollow sites. It is reasonable to assume that one of these two orientations is energetically favorable, so a unique orientation exists (giving the surface a threefold symmetry). Our results require a unique three-fold site but cannot distinguish between hcp or fcc adsorption. A very recent EXAFS study of the low-temperature molecular phase concludes that the Si atoms bond in hcp sites, and supports our conclusions based on the symmetry of the diffraction pattern.⁹

So far, results concerning the adsorption of silane on Cu(111) at 150 K have concentrated on the saturated surface. It was noted from Fig. 5 that during growth there was evidence of surface reordering near saturation coverage. To investigate this observation further, a number of out-of-plane diffraction scans were obtained during growth. Each scan was taken through the same portion of K space, but for a different coverage. Thus the development of a number of diffraction peaks was monitored during growth. Figure 10 shows three diffraction scans obtained at different coverages, as saturation coverage was approached. The magnified section of the uptake curve shows the stage of development of the surface when the scans were obtained. In the first scan, at the lowest coverage, only the specular and $(\bar{1},1)$ peaks are visible. The onset of the $(\bar{1},1)$ peak occurred after approximately one-third of the time it took to form the saturated surface, and the intensity of the peak then gradually increased with coverage. The $\frac{1}{3}$ - and $\frac{2}{3}$ -order peaks appeared as the uptake curve passed through the minimum, i.e., just as

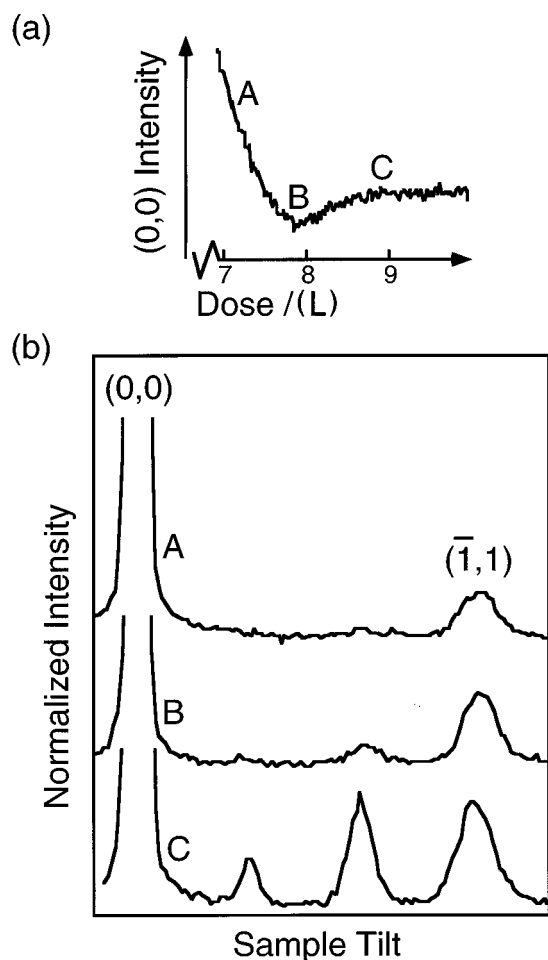


FIG. 10. Diffraction scans obtained for different coverages, during the formation of the silane/Cu(111) surface at 150 K, as saturation coverage is approached. The inset shows a magnified section of the 150-K adsorption uptake curve shown in Fig. 5.

the surface began to reorder. The most striking feature of Fig. 10 is the abruptness of the development of the fractional order diffraction peaks. The fractional order peak intensity increases from zero to maximum (i.e., to saturation of the peak intensity) in only 23% of the time that it took the $(\bar{1},1)$ peak to go from zero intensity to saturation. Thus the process associated with the formation of the fractional order peaks occurs over a much more compressed coverage range than the process associated with the formation of the $(\bar{1},1)$ peak. The other interesting feature highlighted by the diagram is the fact that the formation of the fractional order peaks is associated with the onset of saturation, whereas this is not the case for the $(\bar{1},1)$ peak.

The fact that a $(\bar{1},1)$ diffraction peak is seen at submonolayer coverages suggests that the adsorbed species occupy equivalent sites. It is likely that at coverages well below saturation the adsorbed species form a "lattice gas," with equivalent sites being occupied but with no particular ordering of the species. The abrupt formation of fractional order peaks at saturation implies that the final structure is formed by a sudden ordering of species already present on the surface, rather than the gradual development of areas of the final structure until these areas cover the whole surface at saturation. The sudden ordering of the surface would be consistent

with the hindrance of rotational motion and/or the removal of rotational disorder within the SiH_3 molecules of the proposed surface structure (Fig. 9), as the surface density reaches its saturation value.

The structural investigations of the molecular chemisorbed phase described above were performed at 150 K, which is the lowest surface temperature investigated. However, it was concluded in Sec. III that the heating of the surface after silane adsorption at 150 K (or silane adsorption at higher temperatures) could result in the formation of one of two other molecular chemisorbed structural regimes; see Fig. 1. A limited number of diffraction scans were obtained from these two additional structural regimes. The scans were obtained after producing a saturated surface at 150 K, and then raising the surface temperature T_s to a particular value for 10 s, before cooling the sample back down to 150 K. It was found, in agreement with the temperature-programmed scan of Fig. 1, that structural phases existed in the temperature ranges (a) $T_s < 165$ K, (b) $165 \text{ K} < T_s < 207$ K, and (c) $207 \text{ K} < T_s < 230$ K. Phase (b) had a 4×4 structure, and phase (c) a 3×3 structure. As with regime (a), described earlier in this section, the qualitative features of the diffraction scans from regimes (b) and (c) provided clear evidence of adsorption of species on top of the surface, confirming these regions to be part of the molecular chemisorbed phase, in agreement with the conclusions from Fig. 1.

The RAIRS/EELS data of McCash *et al.*⁶ indicated that the silyl species formed in the lowest-temperature phase dissociates completely at 180 K, leaving ordered atomic hydrogen and disordered elemental silicon bonded to the surface. The hydrogen was thought to desorb at 273 K, leaving the silicon to rearrange into the $(\sqrt{3} \times \sqrt{3})R30^\circ$ structure. In contrast, the results of Ref. 8 suggested that in the intermediate temperature range (~ 180 – 250 K), SiH and H were the species present on the surface. EXAFS data, in this temperature regime, have been interpreted as arising from Si clustering.⁹ At present there are insufficient HAS data to perform a full structural analysis of the intermediate phases; however, the LEED experiments of McCash *et al.* allow some comparison with the HAS data. The LEED data also show the structural phases outlined by Fig. 1, although the precise transition temperatures between phases differ by a few K. There are differences between the structures determined by LEED and HAS. The difference in diffraction patterns observed at $T_s < 165$ K (< 180 K measured by McCash *et al.*) for LEED and HAS has already been discussed. In the 165–207 K regime, McCash *et al.*'s tentative assignment of a fourfold diffraction pattern is confirmed by HAS, which observes a clear 4×4 pattern. However, in the 107–230 K regime there is disagreement. Figure 11 shows a composite pattern from four, out-of-plane, HAS diffraction scans obtained after the Cu(111) surface was exposed to silane to saturation at 150 K, and then annealed to 210 K for 10 s before cooling back down to 150 K. The HAS pattern clearly has 3×3 symmetry, in contrast to the observation of McCash *et al.*, who described their LEED pattern as 3×1 . Even with three domains of a 3×1 structure, the $(\frac{1}{3}, \frac{1}{3})$, $(\frac{1}{3}, \frac{2}{3})$, and $(\frac{2}{3}, \frac{1}{3})$ peaks, seen in Fig. 11, would not be expected in the diffraction pattern. This difference, like that of the 3×3 phase, may be due to the existence of surface hydrogen. At

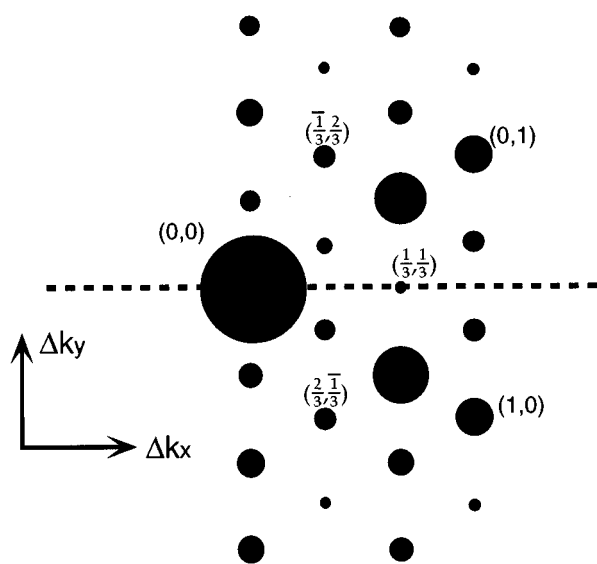


FIG. 11. Helium-atom-scattering diffraction pattern obtained from a Cu(111) surface after exposure to a saturation coverage of silane at 150 K, followed by annealing to 210 K for 10 s. The scattering geometry is the same as in Fig. 3, and the area of the spot is proportional to the integrated intensity of the diffraction peak it represents. The angle of incidence of the helium was 30° at all points along the dotted line, and the beam energy was 71 meV.

present the structures cannot be identified precisely, and further experimental data are required.

VI. CONCLUSIONS

Helium-atom scattering has been used to probe the various temperature regimes of the silane/Cu(111) system. It is found that growth at 400 K results in the formation of a surface alloy phase, whereas for growth below 230 K a molecular chemisorbed phase is formed. A gradual transition from the molecular chemisorbed phase to the surface alloy

phase occurs above 230 K. The surface alloy phase exhibits a $(\sqrt{3} \times \sqrt{3})R30^\circ$ helium diffraction pattern, and has a relatively small corrugation. It is concluded that this phase is formed by the complete molecular dissociation of silane, followed by the desorption of hydrogen and the incorporation of silicon into the surface to give a two-dimensional hexagonal surface alloy (Cu_2Si). The formation of this surface structure is maintained by interlayer bonding, which aids commensurate despite the stretching of in-plane Cu-Si bonds. In contrast, Cu_2Si formation on Cu(001) favors overlayer compression and strong intralayer bonding, and is incommensurate. The competitive energy minimization processes of commensurate and ideal bond length and angle formation associated with the silane/Cu(111) and silane/Cu(001) systems make them interesting candidates for theoretical study.

The molecular chemisorbed phase of the silane/Cu(111) system has three structural regimes. The temperature regime below 165 K exhibits a 3×3 helium diffraction pattern [in contrast to the $(\sqrt{3} \times \sqrt{3})R30^\circ$ structure seen by LEED] with a threefold rotational symmetry. The results indicate that partial molecular dissociation of silane produces ordered silyl moieties, and confirms the presence of SiH_3 on the surface. A $P3m1$ structure with two moieties in the unit cell is consistent with the experimental data. During growth in this regime, ordering of the overlayer into the final surface structure occurred suddenly, at near-saturation coverage. Such behavior is consistent with rotational ordering of SiH_3 molecular fragments when the overlayer density reaches a critical value. The structural regimes at 165–207 and 207–230 K exhibit 4×4 and 3×3 HAS diffraction patterns respectively.

ACKNOWLEDGMENTS

We are grateful to B. Frederick, A. P. Graham, E. M. McCash, and N. V. Richardson for a number of helpful discussions. Rik Balsod is acknowledged for valuable technical assistance. H.G.B. and J.R.B. acknowledge support from EPSRC.

*Present address: Dept. of Chemistry, Rutgers University, NJ 08855-0939.

¹K. Maex, *Physics World* **8**, 35 (1995).

²A. P. Graham, B. J. Hinch, G. P. Kochanski, E. M. McCash, and W. Allison, *Phys. Rev. B* **50**, 15 304 (1994).

³A. P. Graham, E. A. McCash, and W. Allison, *Surf. Sci.* **269/270**, 394 (1992).

⁴A. G. Sault and D. W. Goodman, *Surf. Sci.* **235**, 28 (1990).

⁵L. H. Dubois and B. R. Zegarski, *Surf. Sci.* **204**, 113 (1988).

⁶E. M. McCash, M. A. Chesters, P. Gardner, and S. F. Parker, *Surf. Sci.* **225**, 273 (1990).

⁷T. Asahi, S. Yagi, H. Aga, Y. Takata, Y. Kitajima, T. Yokoyama, and T. Ohta, *Jpn. J. Appl. Phys.* **32**, 380 (1993).

⁸B. C. Wiegand, S. P. Lohokare, and R. G. Nuzzo, *J. Phys. Chem.* **97**, 11 553 (1993).

⁹T. Kanazawa, Y. Kitajima, S. Yagi, A. Imanishi, and T. Ohta, *Surf. Sci.* **357-358**, 160 (1996).

¹⁰R. B. Doak and D. B. Nguyen, *Phys. Rev. B* **40**, 1495 (1989).

¹¹R. J. Wilson, S. Chiang, and F. Salvan, *Phys. Rev. B* **38**, 12 696 (1988).

¹²J. Zegenhagen, E. Fontes, F. Grey, and J. R. Patel, *Phys. Rev. B* **46**, 1860 (1992).

¹³F. J. Walker, E. D. Specht, and R. A. McKee, *Phys. Rev. Lett.* **67**, 2818 (1991).

¹⁴L. H. Dubois and R. G. Nuzzo, *Langmuir* **1**, 663 (1985).

¹⁵A. Reichmuth, Ph.D. thesis, University of Cambridge, 1995.

¹⁶T. Engel and K. H. Rieder, *Structural Studies of Surfaces*, Springer Tracts in Modern Physics Vol. 91 (Springer, New York, 1982), p. 55.

¹⁷F. Greuter and E. W. Plummer, *Solid State Commun.* **48**, 37 (1983).

¹⁸P. Dastoor, M. Arnott, E. M. McCash, and W. Allison, *Surf. Sci.* **272**, 154 (1992).

¹⁹A. Reichmuth, A. P. Graham, H. G. Bullman, W. Allison, and G. E. Rhead, *Surf. Sci.* **307-309**, 34 (1994).

²⁰K. H. Rieder, *Contemp. Phys.* **26**, 559 (1985).

²¹A. P. Graham, E. M. McCash, and W. Allison, *Phys. Rev. B* **51**, 5306 (1995).

²²We note that for hard-wall scattering calculations performed for low angles of incidence and low beam energies, the surface

- corrugation function $\zeta(\mathbf{R})$ cannot be distinguished from its inverse $-\zeta(\mathbf{R})$, and hence hollows in the corrugation function could equally describe “hills” or “hollows” on the real surface (Ref. 23). However, the covalent radius of Si is smaller than that of Cu, so we would expect that the incorporated Si atoms would result in the formation of hollows in the surface corrugation.
- ²³K. H. Rieder, A. Baratoff, and U. T. Hochli, *Surf. Sci.* **100**, L475 (1980).
- ²⁴G. Gross and K. H. Rieder, *Surf. Sci.* **241**, 33 (1991).
- ²⁵W. Li and G. Vidali, *Phys. Rev. B* **47**, 4356 (1992); *Surf. Sci.* **287/288**, 336 (1993).
- ²⁶M. Hohage, T. Michely, and G. Comsa, *Surf. Sci.* **337**, 249 (1995).
- ²⁷B. Poelsema and G. Comsa, *Scattering of Thermal Energy Atoms from Disordered Surfaces*, Springer Tracts in Modern Physics Vol. 115 (Springer, New York, 1989).
- ²⁸E. A. Wood, *Bell Syst. Tech. J.* **43**, 541 (1964).
- ²⁹G. Armand and J. R. Manson, *Phys. Rev. B* **18**, 6510 (1978).
- ³⁰N. Garcia and N. Cabrera, *Phys. Rev. B* **18**, 576 (1978).
- ³¹*Handbook of Chemistry and Physics*, edited by D. R. Lide (CRC, Boca Raton, FL, 1995).
- ³²G. Gross, V. Muller, and K. H. Rieder, *Phys. Rev. B* **44**, 1434 (1991).